A&A 453, 863–868 (2006)
DOI: 10.1051/0004-6361:20054664

Astronomy & Astrophysics

The *K*-band properties of Seyfert 2 galaxies *(Research Note)*

Z. Peng[1], Q. Gu[1,⋆], J. Melnick[2], and Y. Zhao[1]

[1] Department of Astronomy, Nanjing University, Nanjing 210093, PR China
e-mail: [qsgu;yhzhao]@nju.edu.cn
[2] European Southern Observatory, Alonso de Cordova 3107, Santiago, Chile
e-mail: jmelnick@eso.org

Received 8 December 2005 / Accepted 15 March 2006

ABSTRACT

Aims. It is well known that the [O III]λ5007 emission line and hard X-ray (2−10 keV) luminosities are good indicators of AGN activities and that the near and mid-infrared emission of AGN originates from re-radiation of dusty clouds heated by the UV/optical radiation from the accretion disk. In this paper we present a study of the near-infrared K-band (2.2 μm) properties for a sample of 65 Seyfert 2 galaxies.
Methods. By using the AGN/Bulge/Disk decomposition technique, we analyzed the 2MASS K_S-band images for Seyfert 2 galaxies in order to derive the K_S-band magnitudes for the central engine, bulge, and disk components.
Results. We find that the K_S-band magnitudes of the central AGN component in Seyfert 2 galaxies are tightly correlated with the [O III]λ5007 and the hard X-ray luminosities, which suggests that the AGN K-band emission is also an excellent indicator of the nuclear activities at least for Seyfert 2 galaxies. We also confirm the good relation between the central black hole masses and bulge's K-band magnitudes for Seyfert 2s.

Key words. galaxies: active – galaxies: Seyfert – infrared: galaxies – methods: statistical

1. Introduction

In the standard unified scheme, Seyfert 1 and 2 galaxies are intrinsically the same objects; the absence of broad Balmer emission lines in Seyfert 2s is due to the obscuration by a pc-scale dusty torus oriented along the line of sight (Krolik & Begelman 1988; Antonucci 1993). The primary evidence for this model is the detection of polarized broad Balmer emission lines in dozens of Seyfert 2 galaxies, which have betrayed the hidden broad line regions via scattering off electrons and/or dust located above the hole of the torus (Antonucci & Miller 1985; Tran 1995, 2001; Young et al. 1996; Heisler et al. 1997; Moran et al. 2000).

One natural prediction of the unified model is that such a dusty torus surrounding the central engine will absorb the UV/optical radiation from the accretion disk and re-radiate it in the infrared, as the sublimation temperature of graphite grains is in the range 1500−1800 K. According to the Wien law, $T\lambda_{\rm peak}(\mu{\rm m}) = 2898$, the peak wavelength of re-radiation from the dusty torus should be around 2 μm. In fact, it is well known that Seyfert galaxies are strong near and mid-infrared sources (Rieke 1978; Neugebauer et al. 1979). Pier & Krolik (1992) performed the first calculation of thermally re-radiated infrared spectra of the compact dust torus, and found good agreement between the model predictions and observations in Pier & Krolik (1993), which suggested that near infrared emission in Seyfert galaxies mainly arise from the re-radiation of dusty torus heated by UV/optical light from the central engine. Recently, Suganuma et al. (2005) presented reverberation measurements of several well-known Seyfert 1 galaxies by monitoring flux variations in the optical (UBV) and near-infrared (*JHK*) bands. They find a clear time-delayed behavior of the K-band flux variations relative to the V-band. From the flux variation gradients they derive $(H-K)$ color temperatures of 1500−1800 K, and suggest that the bulk of the K-band emission originates from thermal emission of dust grains in the optically thick torus (see also Glass 2004). Thus the K-band emission should also be a good indicator of AGN activity.

The recent, comprehensive Two Micron All Sky Survey (2MASS) has uniformly scanned the entire sky in three near-infrared (NIR) (J 1.25 μm, H 1.65 μm, and K_S 2.17 μm) bands. The point-source sensitivity limits (10σ) are $J = 15.8$ (0.8 mJy), $H = 15.1$ (1.0 mJy), and $K_S = 14.3$ (1.3 mJy) mag. The extended source sensitivity (10σ) is ∼1 mag brighter than the point source limits[1]. The 2MASS public catalog contains >1 000 000 galaxies and thus provides the most comprehensive database for the study of NIR galaxy properties.

In this paper we have performed AGN/Bulge/Disk decomposition for a sample of Seyfert 2 galaxies by using 2MASS K_S-band images in order to derive the near-infrared magnitudes of the central AGNs. In Sect. 2, we present a short description for our sample and present the results of decomposition in Sect. 3. We discuss our results in Sect. 4 and present conclusions in Sect. 5. By using the WMAP data, Spergel et al. (2003) have well determined the Hubble constant to be $H_0 = 71\ {\rm km\,s^{-1}\,Mpc^{-1}}$, which will be used throughout this paper.

⋆ Visiting Scholar, Harvard-Smithsonian Center for Astrophysics, 60 Garden St., Cambridge, MA 02138, USA.

[1] http://www.ipac.caltech.edu/2mass/releases/spr99/doc/test/jarrett2/intro.html

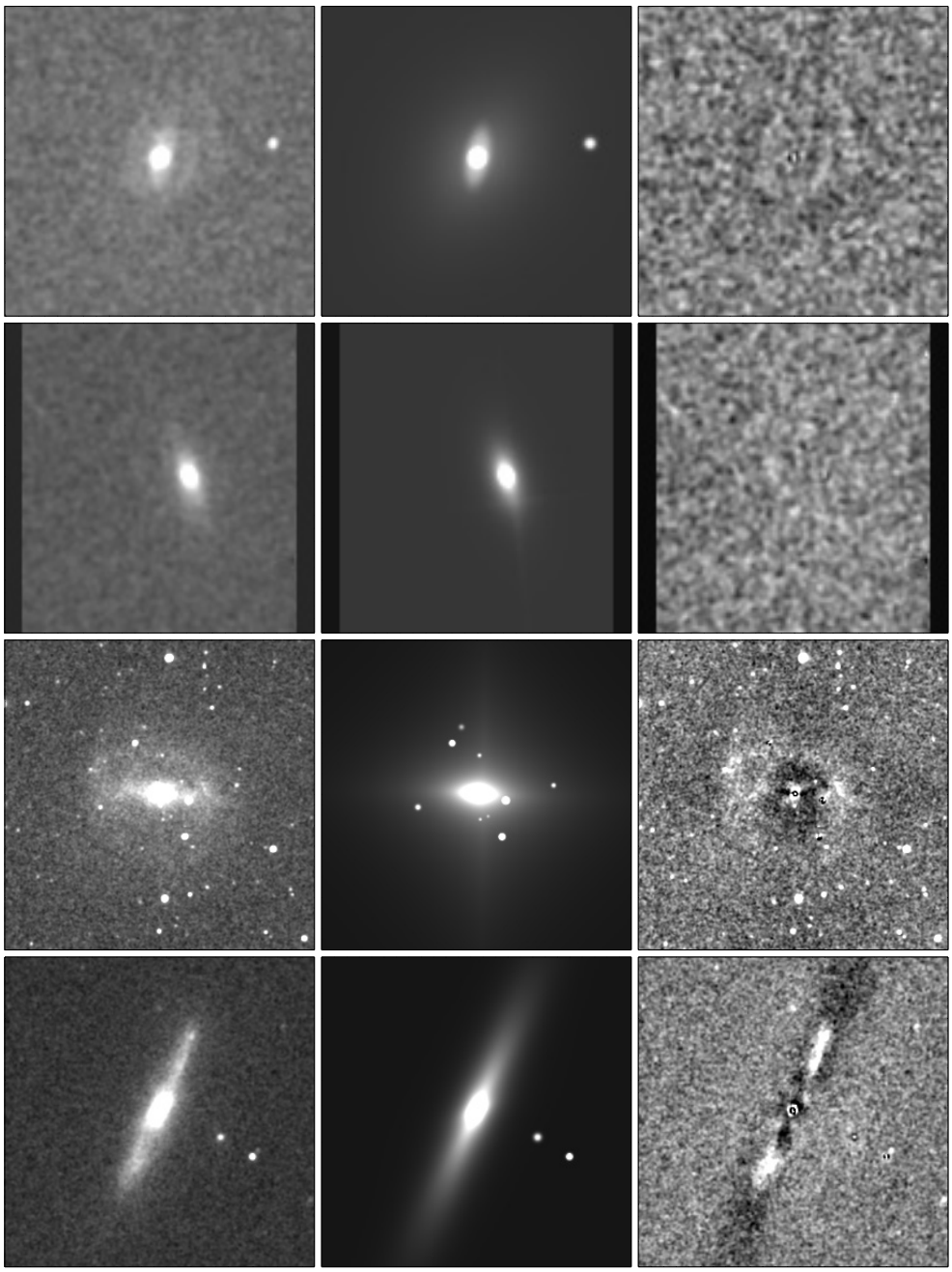

Fig. 1. Results of decomposition. As an example, we only show 4 representative Seyfert 2s with the smallest to the largest χ^2 (NGC 3035, NGC 5252, NGC 5643 and NGC 7582, from *top* to *bottom*). For each source, we show the original image (*left*), the model (*middle*) fitted by GALFIT, and the residual image (*right*).

2. Data

We recently performed a systematic study of a large and homogeneous sample of 65 nearby Seyfert 2 galaxies observable from the southern hemisphere. A full description of the sample selection, observation, and data reduction is presented in Joguet et al. (2001). The star formation history and stellar populations in the central ~200 pc for these Seyfert 2s are derived by means of stellar population synthesis modelling (Cid Fernandes et al. 2004), and Gu et al. (2005) analyzed the "pure" emission line spectra obtained by subtracting the synthetic stellar contribution to derive pure emission-line spectra. Here we use the 2MASS K_S-band images of all Seyfert 2 galaxies in our sample[2], to present a study of NIR properties for these galaxies. The plate scale of the 2MASS K_S-band image is 1.0 arcsec per pixel.

2.1. Light decompositions

We applied the 2-dimensional bulge-disk decomposition program, GALFIT VERSION 2.0.3C (Peng et al. 2002), to the 2MASS K_S-band images of these 65 Seyfert 2 galaxies. Specifically, in order to separate the AGN component, we fitted each galaxy with a combination of a point spread function

[2] http://irsa.ipac.caltech.edu/applications/2MASS/PubGalPS/

Table 1. Properties of Seyfert 2 galaxies.

Galaxy	D (Mpc)	σ (km s^{-1})	$m_{K,\rm AGN}$ (mag)	$m_{K,\rm bulge}$ (mag)	$m_{K,\rm disk}$ (mag)	$\log L_{\rm [OIII]}$ (ergs s^{-1})	$\log L_{2-10\ \rm keV}$ (ergs s^{-1})
ESO 103-G35	56.1	114.0	12.08	11.10	12.29	40.65	42.84
ESO 104-G11	63.9	130.0	11.98	11.51	10.99	40.17	
ESO 137-G34	38.7	133.4	9.63	9.20	8.11	40.80	
ESO 138-G01	38.6	80.0	11.70	10.71	10.53	40.90	>41.51[a]
ESO 269-G12	69.7	160.7	13.19	11.44	10.69	39.53	
ESO 323-G32	67.5	130.6	11.84	10.31	12.60	40.77	
ESO 362-G08	67.4	154.2	11.78	10.07	7.14	40.19	
ESO 373-G29	39.5	92.3	12.64	10.69	10.41	40.21	
ESO 381-G08	46.2	99.7	13.67	10.24	11.30	41.00	
ESO 383-G18	52.4	92.3	12.90	11.99	7.39	40.35	
ESO 428-G14	22.9	119.7	11.28	9.14	13.07	40.52	>40.69[a]
ESO 434-G40	35.0	144.9	10.88	10.18	9.92	40.28	43.11
Fair 334	78.3	104.2	13.08	11.88	10.90	39.93	43.00
Fair 341	67.9	121.9	13.06	10.74	10.93	40.79	43.08
IC 1657	50.5	143.2	12.71	10.30	10.24	38.90	
IC 2560	41.2	143.9	12.22	9.17	10.09	40.46	>40.99[a]
IC 5063	48.0	182.0	12.40	9.41	9.25	40.96	42.92
IC 5135	68.2	143.2	12.17	10.18	10.17	41.15	> 41.45[a]
IRAS F11215-2806	56.9	97.5	14.24	11.93	12.97	40.81	
MCG +01-27-20	49.3	93.9	13.84	11.77	11.53	40.21	
MCG -03-34-64	69.8	155.2	11.24	11.13	10.26	41.86	42.58
Mrk 897	111.2	133.0	12.23	13.34	0	40.13	
Mrk 1210	56.9	114.0	12.69	11.60	10.55	41.05	>42.01[a]
Mrk 1370	103.8	86.1	13.73	13.18	0	40.45	
NGC 424	49.2	142.6	10.34	11.23	10.04	41.78	> 41.55[a]
NGC 788	57.5	162.9	11.93	9.77	0	40.16	
NGC 1068	16.1	143.5	8.02	7.32	6.80	42.00	>41.03[a]
NGC 1125	46.2	104.7	12.05	11.38	10.77	39.84	
NGC 1667	64.0	148.9	12.20	9.63	10.42	39.65	>42.39[a]
NGC 1672	19.0	96.8	11.54	8.95	7.82	38.88	41.21
NGC 2110	32.9	241.5	12.15	8.53	10.02	39.99	42.62
NGC 2979	38.3	112.2	12.62	10.39	10.12	39.29	
NGC 2992	32.5	171.8	11.33	8.96	8.47	40.46	41.76
NGC 3035	61.4	161.4	12.06	12.41	10.03	40.41	
NGC 3081	33.6	133.4	12.28	10.79	9.63	40.55	41.96

(PSF) centered in the image, an inclined exponential disk, and a bulge with a surface brightness profile of $\exp[-(r/r_{\rm s})^{1/n}]$ (Sersic 1968) with the index n constrained to the range of $0.5 \le n \le 5.0$.

Ground-based images usually show near-Gaussian or Moffat-like PSFs (Peng et al. 2002). We generated an analytic profile of PSF for the 2MASS $K_{\rm S}$-band images using the standard tasks in IRAF[3]. Following Jarrett et al. (2000), we used a generalized, radially symmetric exponential function to describe the 2MASS $K_{\rm S}$-band PSF, which is:

$$f(r) = f_0 \exp\left[-\left(\frac{r}{\alpha}\right)^{1/\beta}\right] \quad (1)$$

where f_0 is the central surface brightness, and α and β are free parameters. For the case of the 2MASS survey, we adopted $\beta = 0.5$ and $\alpha = \sqrt{2}\sigma = 1.5''$, where $\sigma = FWHM/2.354$, $FWHM$ is the seeing of the 2MASS images, and $FWHM = 2.5''$ for the $K_{\rm S}$ images[4].

[3] IRAF is distributed by the National Optical Astronomy Observatory, which is operated by the Association of Universities for Research in Astronomy, Inc., under cooperative agreement with the National Science Foundation.

[4] `http://spider.ipac.caltech.edu/staff/roc/2mass/seeing/seesum.html`

Examples of the fitting results are shown in Fig. 1 for 4 representative Seyfert 2s covering the full range of χ^2 (NGC 3035, NGC 5252, NGC 5643, and NGC 7582 with χ^2 of 0.012, 0.013, 0.032, and 0.049, respectively). The standard measurement errors for AGN, bulge, and disk $K_{\rm S}$-band magnitudes are 0.2, 0.3, and 0.5 mag, respectively. For NGC 5643 there appears to be a polar ring left after subtracting the bulge/disk components. This illustrates the high quality of the Bulge/Disk subtraction and may indicate that the ring reflects a dynamical interaction with another galaxy. The currently favored model for the formation of polar rings is suggested to be galactic mergers (Sparke & Cox 2000; Bournaud & Combes 2003; Maccio et al. 2006). For NGC 7582, the residual flux after B/D subtraction is peculiar, which may indicate a warp or some other faint asymmetry in the disk. It is interesting to note that for three objects (Mrk 897, Mrk 1370, and NGC 788 with morphological types of Scd, Sa, and SA(s)0/a, respectively), there seems to be no need for exponential disk components to fit the $K_{\rm S}$-band images.

The decomposed $K_{\rm S}$-band magnitudes of AGN, bulge, and disk are listed in Table 1, where for completeness we also tabulate the stellar velocity dispersions (σ) from Cid Fernandes et al. (2004), and the [O III]λ5007 emission line and the hard X-ray (2−10 keV) continuum luminosities from Gu et al. (2005).

Table 1. continued.

Galaxy	D (Mpc)	σ (km s^{-1})	$m_{K,\rm AGN}$ (mag)	$m_{K,\rm bulge}$ (mag)	$m_{K,\rm disk}$ (mag)	log $L_{\rm [OIII]}$ (ergs s^{-1})	log $L_{2-10\rm keV}$ (ergs s^{-1})
NGC 3281	45.1	160.0	13.24	10.22	8.54	40.26	42.84
NGC 3362	116.7	103.5	13.68	11.05	13.19	41.59	
NGC 3393	52.8	156.7	11.47	10.60	9.83	41.05	>41.13[a]
NGC 3660	51.8	95.5	12.39	10.51	11.57	40.63	
NGC 4388	35.5	110.7	11.26	9.23	9.22	40.98	42.81
NGC 4507	49.9	144.5	11.44	9.51	10.70	41.22	43.33
NGC 4903	69.5	200.4	13.33	10.46	12.41	41.02	
NGC 4939	43.8	154.9	12.18	11.50	9.04	40.75	42.01
NGC 4941	15.6	98.2	11.25	9.01	9.22	39.99	40.95
NGC 4968	41.6	121.1	12.05	10.75	9.44	40.49	>40.92[a]
NGC 5135	57.9	142.6	11.11	10.17	9.98	40.57	>40.91[a]
NGC 5252	97.4	208.9	12.76	10.49	13.44	40.49	43.12
NGC 5427	36.9	100.2	13.16	9.88	9.29	39.90	
NGC 5506	26.1	97.9	9.63	10.74	9.02	40.74	42.94
NGC 5643	16.8	92.9	11.17	7.65	11.25	39.91	>40.65[a]
NGC 5674	105.2	128.5	11.99	12.27	10.21	39.92	43.23
NGC 5728	39.3	155.2	12.43	9.89	8.41	40.82	
NGC 5953	27.7	92.9	12.88	10.03	10.38	39.31	
NGC 6221	20.8	111.4	10.72	8.21	7.96	39.33	
NGC 6300	15.6	99.8	11.22	9.65	6.15	39.44	41.28
NGC 6890	34.1	108.9	12.40	9.35	13.41	40.64	
NGC 7172	36.7	190.0	12.18	10.23	8.89	39.00	
NGC 7212	112.5	167.9	12.47	11.70	9.87	42.01	42.29
NGC 7314	20.0	59.9	12.86	11.43	7.71	39.17	42.29
NGC 7496	23.2	100.7	12.15	9.91	8.87	39.38	41.71
NGC 7582	22.2	132.1	10.13	8.98	7.43	40.39	42.21
NGC 7590	22.5	98.6	11.53	9.63	8.44	39.26	40.86
NGC 7679	72.4	95.9	13.63	10.59	10.27	40.31	42.52
NGC 7682	72.4	152.4	14.65	11.21	9.69	40.74	42.91
NGC 7743	24.1	95.3	11.60	9.98	7.97	38.74	39.56

[a] Compton-thick source with column density $\geq 10^{24}$ cm^{-2}.

3. Results

In the past three decades many attempts were made to establish which are the truly isotropic emissions from Seyfert galaxies. Among various emissions at different wavelengths, the [O III]λ5007 and hard X-ray (2−10 kev) continuum luminosities have been found to show similar distributions for Seyfert 1 and 2 galaxies (Dahari & De Robertis 1988; Keel et al. 1994; Mulchaey et al. 1994; Alonso-Herrero et al. 1997; Kauffmann et al. 2003), indicating isotropic emission and thus making them reliable tracers of the intrinsic nuclear activity. Alonso-Herrero et al. (1997) compared the hard X-ray, the [O III]λ5007, and the small-aperture L-band (3.5 μm) properties of low-redshift PG quasars, Seyfert 1, and 2 galaxies, and they found good correlations between the [O III]λ5007 and L-band properties and between the hard X-ray and L-band properties for Seyfert 1s and PG quasars.

Figure 2 shows the correlation between the $K_{\rm S}$-band absolute magnitudes of our Seyfert 2s with [O III]λ5007 luminosity. The red open squares represent objects where the spectropolarimetric observations detected the polarized broad emission lines (see also Gu et al. 2005), mainly from the compilation by Gu & Huang (2002) plus new observations by Lumsden et al. (2004). As both the AGN $K_{\rm S}$-band absolute magnitude ($M_{K,\rm AGN}$) and [O III]λ5007 luminosity ($L_{\rm [OIII]}$) are well determined, in order to get the best fit between $M_{K,\rm AGN}$ and $L_{\rm [OIII]}$, we used both the ordinary least-square (OLS) bisector method (Isobe et al. 1990)

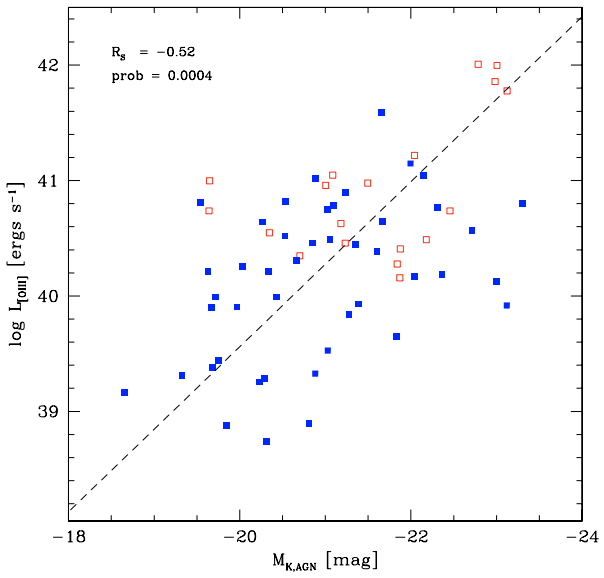

Fig. 2. The AGN $K_{\rm S}$-band absolute magnitude versus [O III]λ5007 luminosity. Red open-square symbols correspond to Seyfert 2s with direct evidence of hidden broad-line regions (HBLR) from spectropolarimetric observations. The dashed line shows a ordinary least square (OLS) bisector fit to the data of slope −0.715±0.051. The Spearman rank-order correlation coefficient ($R_{\rm S}$) is −0.52 and the null probability is 0.0004.

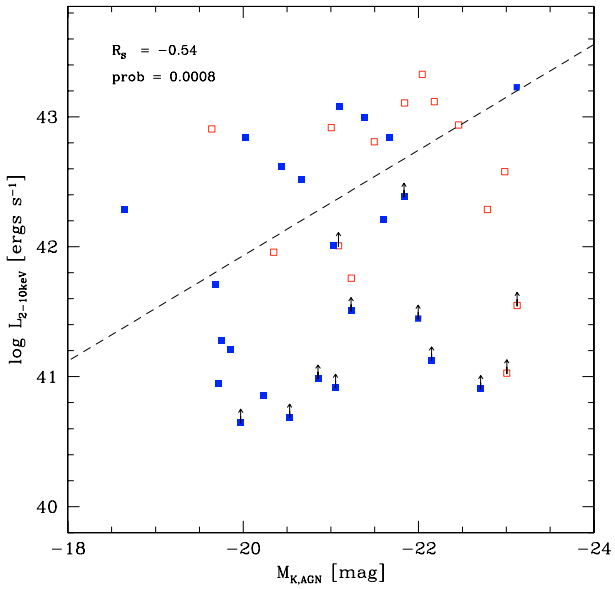

Fig. 3. The AGN K_S-band absolute magnitude versus 2−10 keV hard X-ray luminosity. The dashed line shows an OLS bisector fit to the data of slope −0.406 ± 0.124. The Spearman rank-order correlation coefficient (R_S) is −0.54 and the null probability is 0.0008. Symbols have the same meaning as in Fig. 2.

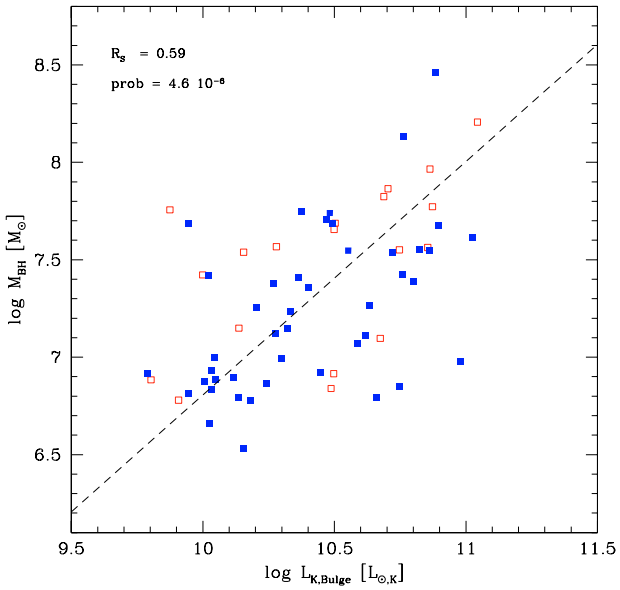

Fig. 4. The bulge's K_S-band absolute magnitude versus the black hole mass. The dashed line shows an OLS bisector fit to the data of slope 1.199 ± 0.080. The Spearman rank-order correlation coefficient (R_S) is 0.59 and the null probability 4.6×10^{-6}. Symbols have the same meaning as in Fig. 2.

and the Buckley-James regression method from the Astronomy Survival Analysis package (ASURV v1.2; Isobe et al. 1985, 1986), and derived the same fitting results, which is $\log L_{[\mathrm{OIII}]} = (-0.715\pm0.051)\,M_{K,\mathrm{AGN}} + (25.260\pm1.092)$. Figure 2 also quotes the Spearman rank-order correlation coefficient (R_S, Press et al. 1992) as −0.52, and a probability of $P_{\mathrm{null}} = 0.0004$ for the null hypothesis of no correlation between $M_{K,\mathrm{AGN}}$ and $L_{[\mathrm{OIII}]}$.

Similarly, Fig. 3 shows the correlation between the AGN K_S-band absolute magnitude versus the hard X-ray 2−10 keV luminosity. Twelve of our Seyferts are Compton-thick sources with column densities larger than 10^{24} cm^{-2}, which are derived by fitting a simple power law with cold absorption to the X-ray spectrum. For Compton-thick objects, the direct hard X-ray continua are completely absorbed, so we cannot estimate their intrinsic hard X-ray luminosities. For these objects, the hard X-ray 2−10 keV luminosities will be taken as lower limits. We have to derive the linear regression using the Buckley-James regression method from ASURV, which is $\log L_{2-10\ \mathrm{keV}} = (-0.406\pm0.124)M_{K,\mathrm{AGN}} + (33.762\pm2.594)$, with a Spearman rank-order correlation coefficient (R_S) of −0.54 and a null probability of $P_{\mathrm{null}} = 0.0008$. As a worst case, if ALL lower limits were detected at their exact lower limit values, the correlation still holds but becomes much steeper. By using the same survival techniques, we derive the best fit to be $\log L_{2-10\ \mathrm{keV}} = (-0.912\pm0.056)\,M_{K,\mathrm{AGN}} + (22.647\pm1.237)$, with the Spearman rank-order correlation coefficient (R_S) of −0.30 and a null probability of $P_{\mathrm{null}} = 0.061$.

Both Figs. 2 and 3 indicate that the AGN K-band magnitudes are tightly correlated with [O III]λ5007 and the hard X-ray (2−10 keV) luminosities, both of which are considered to be good indicators of nuclear activities. Thus it suggests that the AGN K-band magnitude is also a good indicator of AGN activities for Seyfert 2 galaxies. We find in Fig. 2 that Seyfert 2s with hidden broad-line regions clearly have much higher [O III]λ5007 luminosities and higher K_S-band absolute magnitudes, indicating much powerful AGN activities as found by Gu & Huang (2002).

4. Discussion

Since the seeing of 2MASS K_S-band images is rather poor (~2.5″), it is possible that part of the emission from AGN is mixed with that of the bulge. In order to check whether GALFIT did work in this situation, we used the Hubble Space Telescope NICMOS K-band images, which have much better spatial resolution than 2MASS. Fortunately, 3 sources in our sample have NICMOS K-band data: NGC 2110, NGC 2992, and NGC 5643. The AGN magnitudes from NICMOS GALFIT fitting are 12.17, 12.03, and 10.96 mag, respectively. Our values from the 2MASS data are 12.15, 11.33, and 10.69 mag, respectively. For NGC 2110 and NGC 5643, the fitting results are consistent within the typical fitting errors of GALFIT (see Sect. 2) with the NICMOS magnitudes. But for NGC 2992, which is an unabsorbed Seyfert 2 galaxy with a polarized broad Hα emission (Panessa & Bassani 2002; Rix et al. 1990), the magnitude difference is as large as 0.7 mag, which could be evidence of variability or perhaps of an aperture/PSF effect.

4.1. Relation between BH mass and bulge luminosity

It is well known that there is a tight correlation between black hole masses and the bulge properties in spiral galaxies (Magorrian et al. 1998; Gebhardt et al. 2000; Ferrarese & Merritt 2000). Marconi & Hunt (2003) find that NIR bulge luminosities and BH masses are tightly correlated. For those galaxies with accurate BH masses, the spread of such a relation is nearly the same as the famous $M_{\mathrm{BH}} - \sigma$ relation.

Figure 4 shows the relation of bulge K-band absolute magnitudes and BH masses for our sample of Seyfert 2s. The BH mass is derived from the well-known $M_{\mathrm{BH}} - \sigma$ relation,

which is $\log(M_{\rm BH}/M_\odot) = (8.13 \pm 0.06) + (4.02 \pm 0.32) \times \log(\sigma/200\ {\rm km\,s^{-1}})$ (Tremaine et al. 2002), where σ is the stellar velocity dispersion derived by Cid Fernandes et al. (2004). The dashed line is the best fit to the data by means of the OLS bisector method, which is $\log M_{\rm BH}(M_\odot) = (1.199 \pm 0.080) \log(L_{K,{\rm Bulge}}/L_{K,\odot}) - (5.184 \pm 0.831)$. It is very interesting to note that the relation between bulge K-band magnitude and BH mass for Seyfert 2s is nearly the same as that derived for normal galaxies with secure BH mass measurement (see Table 2 in Marconi & Hunt 2003), which shows that host galaxies of Seyfert 2s obey the same relation as normal galaxies. However, our scatter is much larger than that of Marconi & Hunt (2003), the main reason being that BH masses are well-measured in Marconi & Hunt (2003), while we estimate BH masses via the $M_{\rm BH} - \sigma$ relation, and the stellar velocity dispersion was derived by stellar synthesis and thus has larger uncertainties.

5. Conclusion

In this paper, we present a study of NIR properties for a sample of Seyfert 2 galaxies. After decomposing the 2MASS $K_{\rm S}$-band image in the AGN, bulge, and an exponential disk, we derived the $K_{\rm S}$-band magnitudes for each component. We find that the AGN $K_{\rm S}$-band magnitudes are tightly correlated with the luminosities of [O III]λ5007 and the hard X-ray emission, which suggests that the K-band emission is also an excellent indicator of nuclear activity, at least for Seyfert 2 galaxies. We also confirm the good relation between the central black hole masses and bulge's K-band magnitudes.

Acknowledgements. The authors are very grateful to the anonymous referee for his/her instructive comments that significantly improved the content of the paper. We thank Luis C. Ho, Chien Y. Peng, and Leslie K. Hunt for thoughtful discussion and kind help. QGU would like to acknowledge the financial support from the China Scholarship Council (CSC). This work is supported by the National Natural Science Foundation of China under grants 10103001 and 10221001. This research made use of the NASA/IPAC Extragalactic Database (NED), which is operated by the Jet Propulsion Laboratory, California Institute of Technology, under contract with the National Aeronautics and Space Administration. This publication makes use of data products from the Two Micron All Sky Survey, which is a joint project of the University of Massachusetts and the Infrared Processing and Analysis Center/California Institute of Technology, funded by the National Aeronautics and Space Administration and the National Science Foundation.

References

Alonso-Herrero, A., Ward, M. J., & Kotilainen, J. K. 1997, MNRAS, 288, 977
Antonucci, R. R. J. 1993, ARA&A, 31, 473
Antonucci, R. R. J., & Miller, J. S. 1985, ApJ, 297, 621
Bournaud, F., & Combes, F. 2003, A&A, 401, 817
Cid Fernandes, R., Gu, Q., Melnick, J., et al. 2004, MNRAS, 355, 273
Dahari, O., & De Robertis, M. M. 1988, ApJ, 331, 727
Ferrarese, L., & Merritt, D. 2000, ApJ, 539, 9
Glass, I. S. 2004, MNRAS, 350, 1049
Gebhardt, K., Bender, R., Bower, G., et al. 2000, ApJ, 539, L13
Gu, Q., & Huang, J. 2002, ApJ, 579, 205
Gu, Q., Melnick, J., Cid Fernandes, R., et al. 2006, MNRAS, 366, 480
Heisler, C. A., Lumsden, S. L., & Bailey, J. A. 1997, Nature, 385, 700
Isobe, T., Feigelson, E. D., & Nelson, P. I. 1985, BAAS, 17, 573
Isobe, T., Feigelson, E. D., & Nelson, P. I. 1986, ApJ, 306, 490
Isobe, T., Feigelson, E. D., Akritas, M. G., & Babu, G. J. 1990, ApJ, 364, 1041
Jarrett, T. H., Chester, T., Cutri, R., et al. 2000, AJ, 119, 2498
Joguet, B., Kunth, D., Melnick, J., Terlevich, R., & Terlevich, E. 2001, A&A, 380, 19
Kauffmann, G., Heckman, T. M., Tremonti, C., et al. 2003, MNRAS, 346, 1055
Keel, W. C., de Grijp, M. H. K., Miley, G. K., & Zheng, W. 1994, A&A, 283, 791
Krolik, J. H., & Begelman, M. C. 1988, ApJ, 329, 702
Lumsden, S. L., Alexander, D. M., & Hough, J. H. 2004, MNRAS, 248, 1451
Maccio, A. V., Moore, B., & Stadel, J. 2006, ApJ, 636, L25
Magorrian, J., Tremaine, S., Richstone, D., et al. 1998, AJ, 115, 2285
Marconi, A., & Hunt, L. K. 2003, ApJ, 589, L21
Moran, E. C., Barth, A. J., Kay, L. E., & Filippenko, A. V. 2000, ApJ, 540, L73
Mulchaey, J. S., Koratkar, A., Ward, M. J., et al. 1994, ApJ, 436, 586
Neugebauer, G., Oke, J. B., Becklin, E. E., & Matthews, K. 1979, ApJ, 230, 79
Panessa, F., & Bassani, L. 2002, A&A, 394, 435
Peng, C. Y., Ho, L. C., Impey, C. D., & Rix, H. W. 2002, AJ, 124, 266
Pier, E. A., & Krolik, J. H. 1992, ApJ, 401, 99
Pier, E. A., & Krolik, J. H. 1993, ApJ, 428, 124
Press, W. H., Rybicki, G. B., & Hewitt, J. N. 1992, ApJ, 385, 404
Rieke, G. H. 1978, ApJ, 226, 550
Rix, H., Rieke, G., Rieke, M., & Carleton, N. P. 1990, ApJ, 363, 480
Sparke, L. S., & Cox, A. L. 2000, in Dynamics of Galaxies: From the Early Universe to the Present, ed. F. Combes, G. A. Mamon, & V. Charmandaris (San Francisco: ASP), ASP Conf. Ser., 197, 119
Spergel, D. N., et al. 2003, ApJS, 148, 175
Suganuma, M., Yoshii, Y., Kobayashi, Y., et al. 2006, ApJ, 639, 46
Tran, H. D. 1995, ApJ, 440, 565
Tran, H. D. 2001, ApJ, 554, L19
Tremaine, S. D., et al. 2002, ApJ, 574, 740
Young, S., Hough, J. H., Efstathiou, A., et al. 1996, MNRAS, 281, 1206